Lasers in Manufacturing Conference 2015

Energy efficiency in laser rod end melting

Heiko Brüning[a,*], Frank Vollertsen[b]

[a]*BIAS - Bremer Institut für angewandte Strahltechnik, Klagenfurterstr. 2, 28359 Bremen*
[b]*BIAS - Bremer Institut für angewandte Strahltechnik, Klagenfurterstr. 2, 28359 Bremen and University of Bremen*

Abstract

The energetic efficiency of a laser based process, called “laser rod end melting” is investigated. Laser rod end melting allows the generation of spherical geometries at the end of cylindrical rods. After the spherical geometry at the rod end is generated in the master forming stage, this part can be used as a preform for a micro cold forming operation in a subsequent process stage. Within the laser rod end melting process, rods with diameters less than 1 mm are used as wrought material. The presented process is based on the size effect that when scaling down the size of a body, the ratio between surface area and volume is increasing

In this paper, results of the laser rod end melting process concerning the process efficiency with regard to usage of energy are presented. Therefore, the laser rod end melting process is carried out with two different laser beam propagations relative to the rod. For both experimental setups a fiber laser and rods of chromium nickel steel are used. The laser power is measured with a power meter on the work piece surface. A method is presented to determine the energetic efficiency of the laser rod end melting process. It is found that the lateral orientation of the laser beam avoids the defocusing effect so that the energetic efficiency remains constant during accumulation process allowing the total process efficiency to take values of up to 0.45 compared to 0.19 under influence of defocusing effect. Power measurements of the laser beam show a significant deviation between measured laser power and requested power.

Keywords: Laser micro machining; Energy efficiency; Micro forming

* Corresponding author. Tel.: +49-421-21858129; fax: +49-421-21858063.
E-mail address: bruening@bias.de.

1. Introduction

Micro parts can be found in several products of daily life, especially in electronic consumer goods such as smartphones, tablets and digital cameras. A steady increase in the demand of micro parts can be detected for two reasons:

1. Newly invented products are required to fulfil more functions without an increase of total volume of the product. This forces the inner parts, such as screws, contacts or springs to decrease in size.
2. The demand, especially of smartphones such as the iPhone, is increasing.

Over 170 mio. iPhones have been sold in 2014 according to Apple, 2014, each consisting of several micro components which shows the need for mass production of metallic micro parts. Due to certain mechanical requirements, screws or springs are often made of metallic material by cold forming operations. Cold forming operations for example allow an increase in strength of the work piece material compared to machining processes. Another advantage of cold forming processes, especially of bulk metal forming processes, is the high output rate and the realization of small tolerances down to IT7, Lange 2002.

When the outer dimensions of a body are smaller than 1 mm in two directions, parts belong to the "micro range" according to Masuzawa, 2000. When downsizing a body, size effects occur affecting processing the material. This leads to the fact, that knowledge concerning the process parameters in macro range cannot be transferred to micro range accordingly. For example, the conventional mechanical upsetting process allows upset ratios of 2.3 in macro range which is reduced to less than 2 in micro range causing an increase of required upsetting stages if the same final upset ratio is aimed for, Meßner 1998. This characteristic causes an increase of total process time which is detrimental for mass production.

Nomenclature

c_p	specific heat
d_0	diameter of the rod
E_{min}	minimum required energy to generate preform
E_L	laser beam energy based on measured laser power P_L
E_R	laser beam energy based on requested laser power P_R
H_M	latent heat
l_0	length of the rod that is thermally upset
P_L	measured laser power
P_R	requested laser power
T_M	melting temperature
T_0	room temperature
s*	thermal upset ratio
V	volume of preform
α_k	absorption coefficient for abnormal absorption by keyhole
α_n	absorption coefficient for normal absorption
ψ	specific melting volume
ρ	density of rod material

One promising approach to still benefit from the advantages of mechanical upsetting by decreasing the number of required process stages is the laser rod end melting process. A laser beam is focused at the lower end of rod and causes it to melt. The melt forms spherical due to surface tension and solidifies. This part of the rod is now called “preform”. After total cooling, the preform is brought into its final shape by a single stage upsetting operation. Due to the strong influence of surface tension in micro range, the laser rod end melting process allows reaching thermal upset ratios s* >> 200, Stephen and Vollertsen, 2011. As mentioned above, micro parts are generally manufactured in batch sizes of several millions per year. Therefore, the production process has to be efficient with regard to both, use of material and use of energy. Cold forming processes are known to have a high use of material and so has the laser rod end melting process as near net shape or net shape parts can be manufactured such as conical geometries, Brüning and Vollertsen, 2015, comparable to valve lifters. In this paper, results on the energetic efficiency of the laser rod end melting process are presented and discussed.

2. Method

2.1. Generating preforms by laser rod end melting

Generating preforms by laser rod end melting is carried out by applying the power of a laser beam to the lower end of the rod, which is axially fixed. There are two possible options for laser beam incidence to the rod:

1. Coaxial orientation of laser beam and rod. The laser beam interacts with the face surface of the rod end. Both, laser focus and rod are not moved during accumulation process (Fig. 1a, left).
2. Lateral orientation of laser beam and rod. The laser beam interacts with the lateral surface of the rod starting from the rod end and moving upwards according to the axial velocity of the generating preform. Again, the rod is not moved during accumulation process (Fig. 1a, right).

After master forming stage and total cooling, the preform is brought to its final shape by a single stage upsetting operation (Fig. 1b).

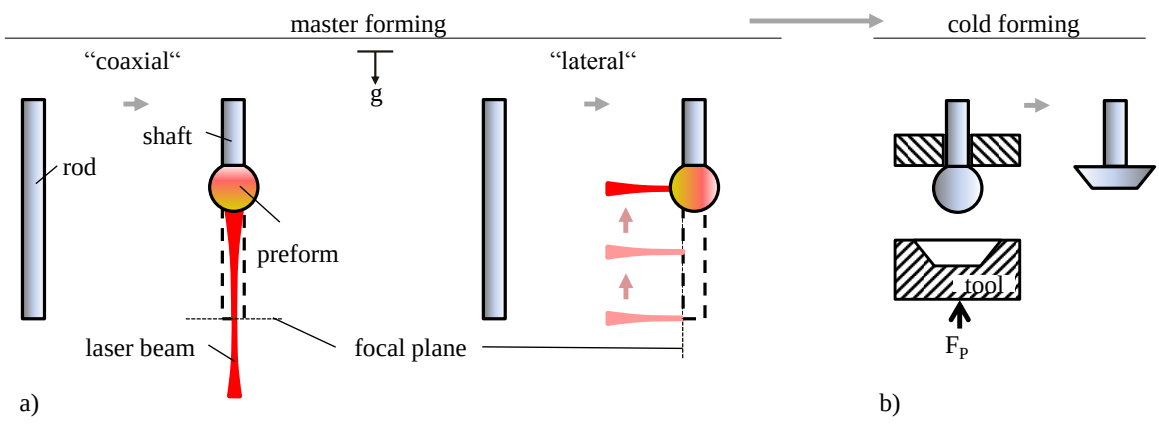

BIAS ID 150194

Fig. 1. Laser rod end melting consists of two process stages: (a) master forming, (b) cold forming. For the master forming stage, two methods are shown, called “coaxial” and “lateral”

In order to characterize the preforms among each other, a dimensionless number called the “thermal upset ratio *s**” is introduced and defined as:

$$s^* := l_0 / d_0 \tag{1}$$

with l_0 as the length of the rod that is melted during the laser rod end melting process and d_0 as the diameter of the rod. The thermal upset ratio is comparable to the upset ratio used within mechanical upsetting operations. The size of the generated preforms is characterized by the diameter. The equatorial diameter is measured five times and then averaged. Assuming that the shape of the preform is spherical, the volume V of the preform can be calculated accordingly.

2.2. Characterization of laser power and beam caustic

The caustic of the laser beam is characterized by a High Power MicroSpotMonitor by Primes GmbH for both strategies of laser beam incidence according to Fig. 1a as different focusing optics are used. The power of the laser beam at the surface of the work piece is measured with a power meter PowerMax USB-150-50C by Coherent Inc. for experimental setup for lateral laser beam incidence. This measuring equipment allows an accuracy of the measurement of ± 2 % of the absolute value and a resolution of 1 mW, Coherent 2013.

2.3. Analytical model for laser energy during accumulation process

For an analysis of the energetic efficiency of the laser rod end melting process, the least required energy to generate a preform is determined. Therefore, the analytical model based on Walther and Vollertsen, 2008, is used. Assuming adiabatic conditions, the least required energy E_{min} equals the energy that is needed to heat up that specific part of the rod from room temperature to melt temperature plus additional latent heat for melting:

$$E_{min} = V \rho \left[c_p \left(T_M - T_0\right) + H_M\right]. \tag{2}$$

If more laser beam energy than E_{min} is required, different reasons could be the case:

- Dissipation of heat by conduction within the rod, radiation or convection by the surface of the preform.
- Some fraction of the laser beam energy is not coupled into the work piece either due to reflection or the beam diameter is larger than the according work piece surface.
- Disagreement between requested laser energy and provided laser energy.
- The temperature of the melt exceeds melting temperature.

2.4. Efficiency of the laser rod end melting process

The efficiency of both strategies for laser rod end melting (Fig. 1a) is calculated based on the analytical model as E_{min} is the lower threshold that is at least required to generate a preform of volume V. According to Fig. 2, two different efficiencies are defined:

1.) the total process efficiency η_Σ

$$\eta_\Sigma := E_{min} / E_R \tag{3}$$

and

2.) the melting efficiency η_m

$$\eta_m := E_{min} / \alpha E_R . \quad (4)$$

To calculate the total process efficiency η_Σ, the laser beam energy that is requested is taken into account. This means, that the absorption coefficient as a consequence of the absorption mechanism has an effect on the total process efficiency. In contrast to that, the melting efficiency η_m only considers that fraction of the requested laser beam energy that is absorbed by the work piece. For normal absorption of laser beam energy on chromium nickel steel, the absorption coefficient is α_n=0.38; if keyhole formation and thus abnormal absorption takes place, the absorption coefficient is α_k=0.85, Hügel and Graf, 2009. So, depending on the position of the system boundary different efficiencies for the same basic process can be found. In Fig. 2, the system boundaries for the total process efficiency η_Σ and the melting efficiency η_m are shown exemplarily for lateral orientation of laser beam and work piece axis.

The specific melting volume ψ is defined as the quotient of preform volume and laser beam energy based on the requested laser beam power:

$$\psi := V / E_R . \quad (5)$$

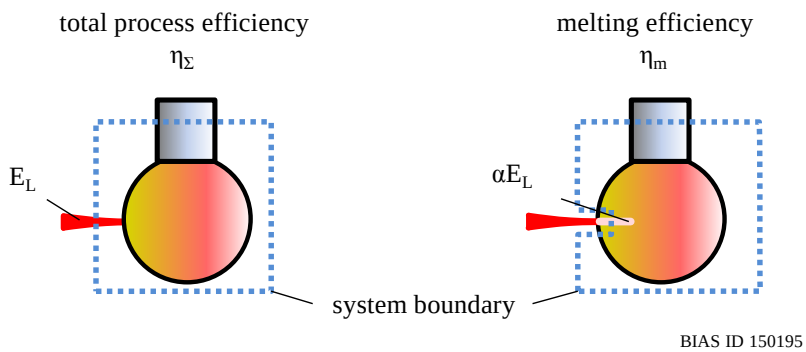

Fig. 2. System boundaries for total process efficiency η_Σ and melting efficiency η_m

3. Experimental setup

Laser rod end melting is carried out with a fiber laser TruFiber300 by Trumpf with a maximum beam power of 300 W according to the specifications. As the position of the rod is kept fixed, different optics are required depending if coaxial or lateral laser beam incidence is desired. For coaxial orientation, a focusing optic with a focal distance of 100 mm is used; the protection window is of BK7 material with a transmittance of 92 %, Laser Components, 2010. As deflection of laser beam is needed to process laser rod end melting with lateral orientation of laser beam and work piece, a 3D-scan head TurboScan AS 30 with linear translation module LTM 20 of Raylase is used. The protection window of the scan head is of quartz glass. According to Laser Components, 2010, the material for the protection window has a transmittance of 93.5 %. The optimum deflection velocity of the laser beam with lateral incidence is applied as characterized by Brüning et al., 2014 representing the optimum total process efficiency η_Σ. For any orientation “coaxial” or “lateral”, the surface interacting with the laser beam is initially placed in focal plane. The rod material is austenitic chromium nickel steel 1.4301 (similar to AISI 304, X5CrNi18-10) with diameter d_0 of 0.3 mm,

0.4 mm and 0.5 mm. For each set of process parameters, experiments are carried out without repetition. In any case during master forming stage, the according surface of the work piece is larger than the beam diameter which means that no fraction of the beam passes the work piece without interaction.

4. Results

4.1. Beam characteristic

The beam caustic is an important characteristic for the determination and the interpretation of the energetic efficiency of the laser rod end melting process. The relevant parameters concerning this matter for coaxial and lateral orientation of laser beam and work piece can be found in Table 1. The different values derive from the beam shaping optics.

Table 1. Beam caustic for focusing optic with focal distance of 100 mm and for 3D-scan head. Measurements are carried out with requested laser power of 100 W

beam source		TruFiber 300			
wave length	nm	1085			
		"coaxial"		"lateral"	
beam shaping optic		fixed focusing optic		3D-scan head	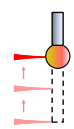
focus radius	µm	11.0		25.5	
Rayleigh length	mm	0.26		1.44	
divergence angle	mrad	85.3		35.3	
M^2		1.35		1.33	

For investigations concerning energetic efficiency of laser rod end melting process, the power of the laser beam on the surface of the work piece is measured by use of the 3D-scan head and a power meter. Fig. 3 shows the measured power P_L plotted against the requested power P_R which is typed in the control panel. The measured power lies always below the requested power.

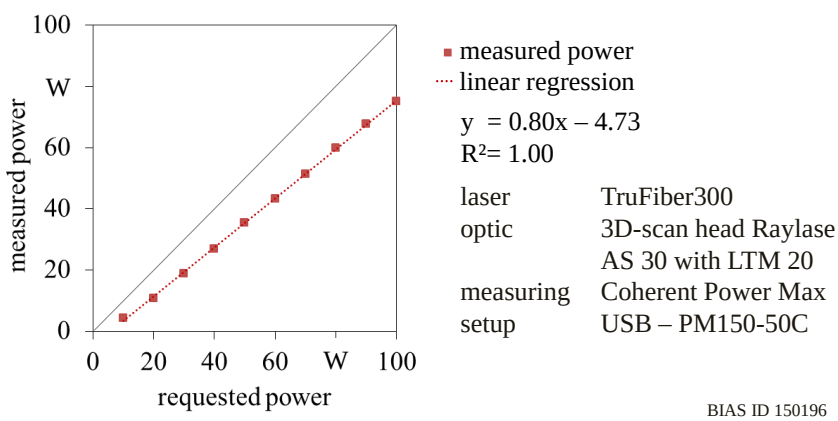

Fig. 3. Measured laser power plotted against requested laser power for Trumpf TruFiber 300 with Raylase 3D-scan head

A linear regression curve with a gradient of 0.80 and an intercept of -4.73 W shows a good correlation with the measured power. It can be stated that the laser power on the surface of the work piece is approximately 20 % lower than requested which could be a consequence of absorption along the beam path.

4.2. Energy efficiency

For both strategies of laser beam incidence, “coaxial” and “lateral”, the specific melting volume ψ is calculated which gives information about the volume of a preform that can be generated with 1 J of requested laser beam energy, Eq. (5). The specific melting volume ψ is plotted against the thermal upset ratio s^* in Fig. 4. It can be derived that for thermal upset ratios $s^* \leq 3$ the specific melting volume is independent of the method which is used to generate the preform. This behavior changes with increasing thermal upset ratio. For coaxial orientation, the specific melting volume decreases rapidly to values of $\psi_A = 0.02$ mm³/J and remains almost constant further on. In contrast, the specific melting volume which is achieved with lateral orientation is $\psi_B \approx 0.05$ mm³/J and is independent of thermal upset ratio s^* but a wider range of scatter is observed. The wider scatter of specific melting volume indicates that the process is not as stable as the process carried out with coaxial orientation. For both orientation of laser beam and work piece, the specific melting volume is independent of the rod diameter. Exemplarily, the intensity on the surface of the preform of a rod with $d_0 = 0.4$ mm is also plotted in Fig. 4 for coaxial orientation and requested laser power of $P_R = 140$ W. It is shown that the intensity decreases to values below 10^7 W/cm² for thermal upset ratios $s^* > 3$.

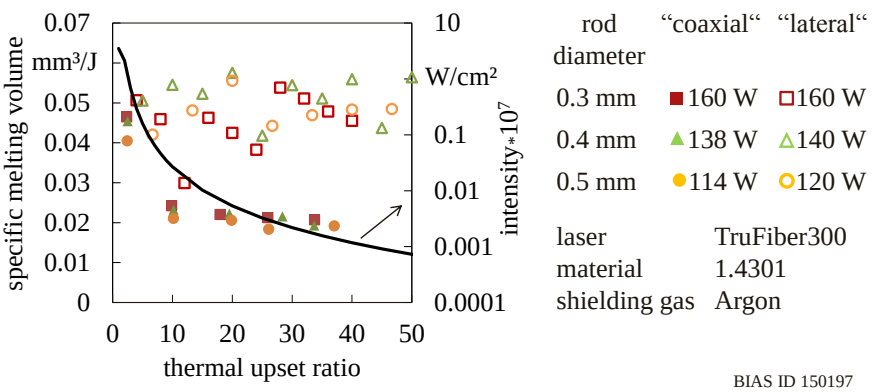

Fig. 4. Specific melting volume ψ plotted against the thermal upset ratio s* for laser rod end melting with coaxial and lateral orientation for chromium nickel steel

To determine the total process efficiency as well as the melting efficiency for coaxial and lateral orientation of laser beam and work piece, the specific melting volume ψ is related to the minimum required energy according to Eq. (3) and Eq. (4). It is clearly shown that there is a linear correlation between the specific melting volume and the total process efficiency which can be seen by comparing the associated curves in Fig. 4 and Fig. 5. As the rod diameter does not influence the specific melting volume and thus not the efficiency, the different rod diameters are not indicated separately in Fig. 5 to increase clearness of the graphic. It is observed that the total process efficiency is almost independent of thermal upset ratio for laser rod end melting by lateral orientation as the gradient of the regression is 0.0007. The intercept of the linear

regression is $\eta_\Sigma = 0.34$. The total process efficiency in coaxial orientation is dependent of the thermal upset ratio. For thermal upset ratios $s^* \leq 3$, a total process efficiency $\eta_\Sigma \approx 0.34$ is observed. This value decreases with increasing thermal upset ratio. For thermal upset ratios $10 \leq s^* \leq 40$, a linear trend of total process efficiency is observed with a gradient of -0.0010.

A major difference between coaxial and lateral orientation is the distance between the work piece surface and the focal plane. For "coaxial", this value is increasing with increasing thermal upset ratio which causes a decrease of beam intensity, given that the laser power is constant. If the work piece surface is in focal plane, the intensity is high enough for abnormal absorption of laser beam energy. As the Rayleigh length of the optic setup is << 1 mm (Table 1), the intensity on the work piece surface falls below the threshold required for abnormal absorption for thermal upset ratios $s^* > 3$.

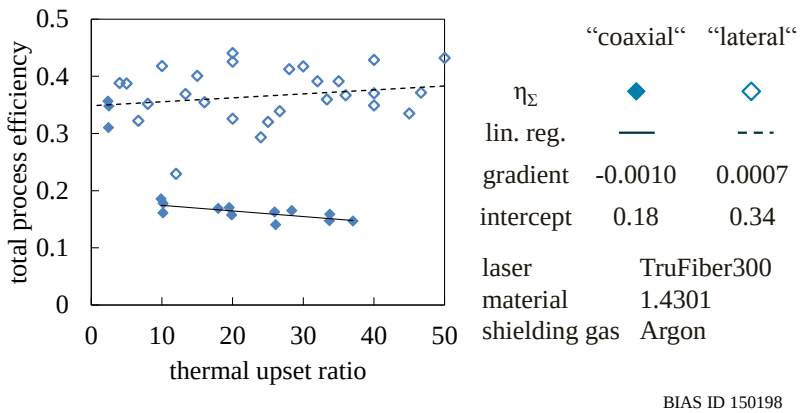

Fig. 5. Total process efficiency of laser rod end melting process for coaxial and lateral orientation with fiber laser TruFiber300.

For calculating the melting efficiency η_m, the mechanism of laser beam absorption is also taken into account. If normal absorption takes place, which is according to the laser intensity only the case for laser rod end melting with coaxial orientation of laser beam and symmetric axis of the work piece and thermal upset ratios $s^* \geq 3$, an absorption coefficient of $\alpha_n = 0.38$ is assumed. For any other condition, abnormal absorption takes place due to beam intensities $\geq 2 \cdot 10^7$ W/cm² with an assumed absorption coefficient $\alpha_k = 0.85$.

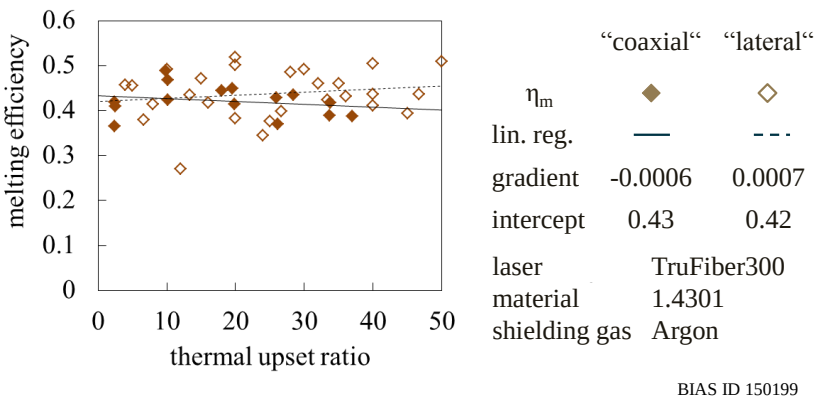

Fig. 6. Melting efficiency of laser rod end melting process for coaxial and lateral orientation

Fig. 6 shows the melting efficiency plotted against the thermal upset ratio for “coaxial” and “lateral”. It can be derived that for both methods the melting efficiency takes values between $0.35 \leq \eta_m \leq 0.53$ if one outlier (12|0.27) is neglected. The trend line for “coaxial” has a gradient of -0.0006 which is very close to 0 just as the gradient of the trend line for “lateral” with +0.0007. The intercept of the trend lines is 0.42 and 0.43, respectively. These values show that melting efficiency of both methods is very similar.

5. Discussion

A fiber laser is used to process two different methods of laser rod end melting. The measured power on the surface of the work piece is ~20 % less than the laser power requested by the control panel for the experimental setup with a 3D-scan head. The significant difference between the measured laser power and the requested laser power might be (among others) the result of the following influences:

- absorption by optical elements in beam propagation e.g. lenses and protection window
- mechanical coupling between fiber and collimator
- inaccuracy of the measuring tool
- adjustment of laser beam source,

which are discussed in the following. As stated above, the transmittance of the protection window is 93.5 %, reducing significantly the measured laser power. The influence of optical elements such as lenses can be neglected as transmittance of 99.95% is given for the lens material according to Laser Components, 2010. Even though the optical beam path is guided by 9 lenses between the end of the fiber and the protection window, these losses only end up to 0.45 %. The inaccuracy of the power measuring tool is ± 2 % of the measured value. Adding the percentaged influences, the laser power is reduced to a maximum of 9 %. As a consequence, either the adjustment of the laser beam source or the mechanical coupling between fiber and collimator is found to be responsible for a power loss of approximately 10 %. According to Kerstens et al. 2003, this seems reasonable as in that case a loss of laser power of even 24 % was detected within the fiber. As both elements, fiber and collimator, are used for either orientation “coaxial” and “lateral” and the influence of the number of lenses in the beam path seems negligible, the linear regression measured for the experimental setup for “lateral” is also reasonably applicable for “coaxial” orientation of laser beam and work piece. The observed correlation between measured laser power and requested laser power is linear with $R^2 = 1$ for $10\ \text{W} \leq P_L \leq 100\ \text{W}$, therefore an extrapolation to higher laser power seems acceptable. It is relevant to measure the delivered laser beam power because the power losses within the beam path (and thus the deviation between requested and delivered power) have an effect on the absolute value of the calculated process efficiency of the laser rod end melting process.

Regarding the thermal balance during accumulation process, it could be possible, that the accumulating preform by coaxial orientation of laser beam and work piece axis might get much hotter than if accumulated with lateral beam incidence as melting of the rod can only be caused by overheating of the melt. For this reason, two different system boundaries were defined to determine on one hand the total process efficiency and on the other hand the melting efficiency. As expected, the total process efficiency is higher for “lateral” and thermal upset ratios $s^* \geq 3$ due to abnormal absorption. Nevertheless, for very small thermal upset ratios where abnormal absorption also takes place with coaxial orientation, the total process efficiency is equal with respect to measuring inaccuracies. If the absorption mechanism is taken into account, both accumulating methods show the same melting efficiency if the same requested laser power is applied. This means that a preform “C” processed with coaxial orientation uses a fraction of the incoupled energy which is of the same amount than that the preform “L” would use with lateral orientation. This could be an indication, that the preforms of both orientations “coaxial” and “lateral” reach approximately the same

average temperature during accumulation process as the same amount of incoupled laser beam energy is not used for melting the material.

The lateral orientation of work piece and laser beam enables a higher total process efficiency in terms of usage of energy for thermal upset ratios $s^* \geq 3$, making it less time consuming which can be an important factor for industrialized mass production as metallic micro parts are usually manufactured in batch size of several millions per year.

6. Summary

Two different methods to process laser rod end melting are presented and compared in terms of energetic efficiency. It is shown that a lateral incidence of laser beam on the lateral surface of the rod allows constantly high total process efficiency independent of thermal upset ratio because the surface of the work piece remains in focal plane so that abnormal absorption is achieved throughout the whole process avoiding the defocussing effect. The melting efficiency (which takes the differences in the absorption coefficient into account) for both laser rod end melting processes is nearly the same which could be an indication that the average temperatures of the melt during accumulation process are similar.

Acknowledgements

The authors gratefully acknowledge the financial support by Deutsche Forschungsgesellschaft (DFG, German Research Foundation) for subproject A3 “Stoffanhäufen” within the SFB 747 (Collaborative Research Centre) “Mikrokaltumformen - Prozesse, Charakterisierung, Optimierung”. The authors would like to thank Stefan Veenaas for his support.

References

www.apple.com, 2014. Gathered information from Apple Reports Quarter Results, access 19.12.2014.

Lange, K., 2002. Umformtechnik - Handbuch für Industrie und Wissenschaft, Band 1. Berlin: Springer-Verlag.

Masuzawa, T., 2000. State of the Art of Micromachining, Keynote Paper, Annals of the CIRP, 49(2), 473-488.

Meßner, A., 1998. Kaltmassivumformung metallischer Kleinstteile: Werkstoffverhalten, Wirkflächenreibung, Prozessauslegung, PhD-thesis, Meisenbach Verlag, ISBN 978-3875251005.

Stephen, A., Vollertsen, F., 2011. Influence of the Rod Diameter on the Upset Ratio in Laser-based Free Form Heading. Steel Research International, Special Edition pp. 220-223.

Brüning, H., Vollertsen, F., 2015. Form filling behaviour of preforms generated by laser rod end melting. Annals of the CIRP, in press.

Coherent, 2013. Laser Measurement and Control - Product Catalog, Coherent Inc., Portland, Wilsonville, OR 97070.

Vollertsen, F., Walther, R., 2008. Energy balance in laser-based free form heading. Annals of the CIRP, 57(1), 291-294.

Hügel, T., Graf, T., 2009. Laser in der Fertigung. Vieweg und Teubner, Wiesbaden.

Laser Components, 2010. Optimale Materialauswahl, Dokument 07/10/IF/V1/lco/tipps/optimal_material.pdf.

Brüning, H., Veenaas, S., Vollertsen, F., 2014. Determination of axial velocity of material accumulation in laser rod end melting process, Proceedings of the 4th International Conference on Nanomanufacturing (nanoMan 2014), 8 – 10 July, 2014, eds.: F. Fang, E. Brinksmeier, O. Riemer, Paper F1-3 (USB-Stick).

Kersten, N.F.H., Richardson, I.M., Stoop, B.T.J., 2003. High Power Diode Laser Welding of AA2024 and AISI316L, International Congress on Applications of Lasers & Electro–Optics, ICALEO, Paper 207, 2003.